Available online at www.sciencedirect.com

ScienceDirect

Polyhedron 26 (2007) 2482–2492

POLYHEDRON

www.elsevier.com/locate/poly

Synthetic and X-ray diffraction studies of borosiloxane cages [R′Si(ORBO)$_3$SiR′] and the adducts of [Bu^{t}Si{O(PhB)O}$_3$SiBu^t] with pyridine or *N*,*N*,*N*′,*N*′-tetramethylethylenediamine

George Ferguson [a,*], Simon E. Lawrence [b], Lorraine A. Neville [b], Brian J. O'Leary [b], Trevor R. Spalding [b,*]

[a] *School of Chemistry, The University of St. Andrews, Fife KY16 9ST, UK*
[b] *Department of Chemistry, University College Cork, National University of Ireland, Cork, Ireland*

Received 8 November 2006
Available online 20 January 2007

Abstract

Eleven borosiloxane [R′Si(ORBO)$_3$SiR′] compounds where R′ = Bu^t and R = Ph (**1**), 4-PhC$_6$H$_4$ (**2**), 4-Bu^{t}C$_6$H$_4$ (**3**), 3-NO$_2$C$_6$H$_4$ (**4**), 4-CH(O)C$_6$H$_4$ (**5**), CpFeC$_5$H$_4$ (**6**), 4-C(O)CH$_3$C$_6$H$_4$ (**7**), 4-ClC$_6$H$_4$ (**8**), 2,4-F$_2$C$_6$H$_3$ (**9**), and R′ = *cyclo*-C$_6$H$_{11}$ and R = Ph (**10**), and 4-BrC$_6$H$_4$ (**11**) have been synthesized and characterized by spectroscopic (IR, NMR), mass spectrometric and, for compounds where R′ = Bu^t and R = 4-PhC$_6$H$_4$ (**2**), 4-Bu^{t}C$_6$H$_4$ (**3**), 3-NO$_2$C$_6$H$_4$ (**4**), CpFeC$_5$H$_4$ (**6**) and 2,4-F$_2$C$_6$H$_3$ (**9**), X-ray diffraction studies. These compounds contain trigonal planar RBO$_2$ and tetrahedral R′SiO$_3$ units located around 11-atom "spherical" Si$_2$O$_6$B$_3$ cores. The dimensions of the Si$_2$O$_6$B$_3$ cores in compounds **2**, **3**, **4**, **6** and **9** are remarkably similar. The reaction between [Bu^{t}Si{O(PhB)O}$_3$SiBu^t] (**1**), and excess pyridine yields the 1:1 adduct [Bu^{t}Si{O(PhB)O}SiBu^t]. NC$_5$H$_5$ (**12**) while the reaction between **1** and *N*,*N*,*N*′,*N*′-tetramethylethylenediamine in equimolar amounts affords a 2:1 borosiloxane:amine adduct [Bu^{t}Si{O(PhB)O}$_3$SiBu^t]$_2$ · Me$_2$NCH$_2$CH$_2$NMe$_2$ (**13**). Compounds **12** and **13** were characterised with IR and (^{1}H, ^{13}C and^{11}B) NMR spectroscopies and the structure of the pyridine complex **12** was determined with X-ray techniques.

© 2006 Elsevier Ltd. All rights reserved.

Keywords: Borosilicate; Borosiloxanes; Cage compounds; X-ray diffraction; Structures

---

1. Introduction

The chemistry of three-dimensional cage species containing only main group elements bonded by two center–two electron bonds is notable for the large number of silesesquioxanes [(RSi)$_8$O$_{12}$] which have been reported [1]. For cages containing main group 13 elements, aluminium systems are perhaps the most studied with aluminium–nitrogen compounds predominant [2]. Boron containing species are relatively rare [3] but previously reported borosiloxane cage compounds that have been structurally characterised include [Bu^{t}Si{O(4-BrC$_6$H$_4$B)O}$_3$SiBu^t] which contains the 11-atom "spherical" B$_3$Si$_2$O$_6$ core [4], [B(OSiPh$_2$SiPh$_2$O)$_3$B] with a "cylindrical" B$_2$Si$_6$O$_6$ core [5], "cube-based" [(Bu^{t}Si)$_4$(4-RC$_6$H$_4$B)$_4$O$_{10}$] species where R = (CH$_2$=CH) [6] or Br [7] which have B$_4$Si$_4$O$_{10}$ cores, and silesesquioxane-based species which contain "cube-based" BSi$_7$O$_{12}$ units [8]. One overall intention of the work carried out by our group [3–7] was to synthesise a variety of three-dimensional structures which could be reacted further to produce new molecular scaffolds in a controlled way. We now report the extension of the chemistry of the

---

[*] Corresponding authors.
E-mail addresses: gf3@st-andrews.ac.uk (G. Ferguson), t.spalding@ucc.ie (T.R. Spalding).

0277-5387/$ - see front matter © 2006 Elsevier Ltd. All rights reserved.
doi:10.1016/j.poly.2006.12.045

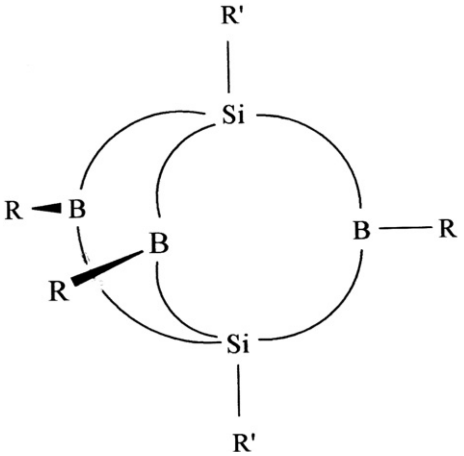

Diagram 1.

"spherical" cage borosiloxanes with the syntheses of 11 analogues of [R′Si(OBRO)$_3$SiR′] with a wide variety of R groups, Diagram 1.

The details of the structures of five of these compounds have been determined with X-ray crystallography. Additionally, we have studied the reactions between [Bu^{t}Si{O(PhB)O}$_3$SiBu^t] (**1**) and (a) pyridine or (b) *N*,*N*,*N*′,*N*′-tetramethyl-ethylenediamine and established the solid-state structure of the adduct [Bu^{t}Si{O(PhB)O}SiBu^t] · NC$_5$H$_5$ (**12**).

2. Results and discussion

2.1. Syntheses and structural studies of [R′Si(ORBO)$_3$SiR′] borosiloxanes *1* to *11*

All the borosiloxane cages with the formulae [R′Si(ORBO)$_3$SiR′] were synthesised in a Dean-Stark apparatus by water elimination reactions between R′Si(OH)$_3$ (R′ = Bu^t or *cyclo*-C$_6$H$_{11}$) and boronic acids RB(OH)$_2$ in a 2:3 molar ratio in toluene solution heated at the reflux temperature, Eq. (1). In general the *tert*-butyl compounds were isolated in 30–40% higher yields than the corresponding *cyclo*hexyl derivatives with the same R groups.

$$2R'Si(OH)_3 + 3RB(OH)_2 \rightarrow [R'Si(ORBO)_3SiR'] \quad (1)$$

where R′ = Bu^t and R = Ph (**1**), 4-PhC$_6$H$_4$ (**2**), 4-Bu^{t}C$_6$H$_4$ (**3**), 3-NO$_2$C$_6$H$_4$ (**4**), 4-CH(O)C$_6$H$_4$ (**5**), CpFeC$_5$H$_4$ (**6**), 4-C(O)CH$_3$C$_6$H$_4$ (**7**), 4-ClC$_6$H$_4$ (**8**), 2,4-F$_2$C$_6$H$_3$ (**9**), and R′ = *cyclo*-C$_6$H$_{11}$ and R = C$_6$H$_5$ (**10**), and 4-BrC$_6$H$_4$ (**11**).

An alternative route via the reactions between *tert*-butyltrichlorosilane or *cyclo*hexyltrichlorosilane and boronic acids in the presence of an amine, either Et$_3$N or aniline, afforded the products **1** to **9** in 5–10% lower yields and compounds **10** and **11** in ca. 30% lower yields. Attempts to use phenyl- or tolyltrichlorosilane reagents afforded boroxines as the only characterisable products.

Initial characterisation of **1**–**11** by chemical analysis was followed by spectroscopic (FT-IR, NMR) and, in some cases, mass spectrometric analysis. For the compounds with R′ = Bu^t and R = 4-PhC$_6$H$_4$ (**2**), 4-Bu^{t}C$_6$H$_4$ (**3**), 3-NO$_2$C$_6$H$_4$ (**4**), CpFeC$_5$H$_4$ (**6**), and 2,4-F$_2$C$_6$H$_3$ (**9**), single-crystal X-ray diffraction studies were carried out. A summary of crystal data for these compounds is given in Section 4.

2.2. Crystal and molecular structures of [Bu^{t}Si{O(4-PhC$_6$H$_4$B)O}$_3$SiBu^t] (2), [Bu^{t}Si{O(4-Bu^{t}C$_6$H$_4$B)O}$_3$SiBu^t] (3), [Bu^{t}Si{O(3-NO$_2$C$_6$H$_4$B)O}$_3$SiBu^t] (4), [Bu^{t}Si{O(CpFeC$_5$H$_4$B)O}$_3$SiBu^t] (6), and [Bu^{t}Si{O(2,4-F$_2$C$_6$H$_3$B)O}$_3$SiBu^t] (9)

Comparison of the structures of compounds [Bu^{t}Si(OBRO)$_3$SiBu^t] where R = 4-PhC$_6$H$_4$ (**2**), 4-Bu^{t}C$_6$H$_4$ (**3**), 3-NO$_2$C$_6$H$_4$ (**4**), CpFeC$_5$H$_4$ (**6**) and 2,4-F$_2$C$_6$H$_3$ (**9**) reveals that the structural details of the Si$_2$O$_6$B$_3$ cages are remarkably similar, Table 1.

All five compounds contain two tetrahedral Bu^{t}SiO$_3$-units and three trigonal planar RBO$_2$-units held together by an 11-atom Si(OBO)$_3$Si framework. Figs. 1–3 show ORTEP views of molecules with R = 4-PhC$_6$H$_4$ (**2**), 4-Bu^{t}C$_6$H$_4$ (**3**) and CpFeC$_5$H$_4$ (**6**) from a general perspective.

The structures of compounds **2** and **6** are shown viewed along the axes passing through both silicon atoms in Figs. 4 and 5, respectively. The *tert*-butyl groups attached to the silicon atoms in compounds **2** and **6** are in "eclipsed" arrangements. The same structural motif is found in **3**, **4**, **6** and **9**.

The C$_6$-rings attached to the boron atoms in **2** and **3** are arranged in a "paddlewheel" formation, see Fig. 4, and are almost co-planar with the adjacent Si–O–B–O–Si bonded sequence. The same structural motif was observed in **3**, **4**, and **9**, and in the compound [Bu^{t}Si{O(4-BrC$_6$H$_4$B)O}$_3$SiBu^t] [4]. A similar situation is observed in the ferrocenyl compound [Bu^{t}Si{O(CpFeC$_5$H$_4$B)O}$_3$SiBu^t] (**6**), where the C$_5$H$_4$ ring is almost co-planar with the attached borosiloxane group, Fig. 5. The reason for the preference for co-planarity may reside in a partial overlap of the π system of the aromatic C$_6$-ring and some delocalised bonding in the Si–O–B–O–Si sequence. However, it is also possible that the co-planarity is due to "crystal packing" forces. It is interesting to note that in the case of **6** the ferrocenyl groups are not all arranged to give a pseudo-D_{3h} molecular symmetry. The reasons are unclear but may be due either to weak intramolecular H···π–C$_5$H$_5$ ring interactions or more general "crystal packing" forces.

The B–O lengths in **2**, **3**, **4**, **6** and **9** range from 1.348(5) to 1.380(4) and are at the upper end of the reported range for trigonal boron species with Si–O–B bonds i.e. 1.313(2) in (OBF)(OSiBu$^t_2$)$_2$(OSiMe$_2$) (**13**) [9] to 1.374(7) Å in [B(OSiPh$_2$SiPh$_2$O)$_3$B] (**14**) [5]. They are similar to B–O distances in the previously reported spherical cage [Bu^{t}Si{O-(4-BrC$_6$H$_4$B)O}$_3$SiBu^t] (**15**) [4], which were

Table 1
Selected bond distance (Å) and angle (°) data for $[\mathrm{Bu}^t\mathrm{Si(OBRO)}_3\mathrm{SiBu}^t]$ where R = 4-$\mathrm{PhC_6H_4}$ (**2**), 4-$\mathrm{Bu}^t\mathrm{C_6H_4}$ (**3**), 3-$\mathrm{NO_2C_6H_4}$ (**4**), $\mathrm{CpFeC_5H_4}$ (**6**) and 2,4-$\mathrm{F_2C_6H_3}$ (**9**)

Compound	**2**	**3**	**4**	**6**	**9**
Range of Si–O distances	1.615(2)–1.6212(19)	1.613(3)–1.624(3)	1.603(3)–1.631(3)	1.621(3)–1.637(2)	1.620(4)
Mean Si–O	1.620(2)	1.620(3)	1.620(3)	1.628(3)	1.620(4)
Range of B–O distances	1.353(4)–1.380(4)	1.348(5)–1.376(6)	1.354(5)–1.370(5)	1.359(4)–1.373(5)	1.372(6)
Mean B–O	1.365(4)	1.364(6)	1.364(5)	1.369(5)	1.372(6)
Mean B–C	1.553(4)	1.546(6)	1.559(6)	1.541(5)	1.544(12)
Mean Si–C	1.833(3)	1.841(5)	1.829(4)	1.851(4)	1.838(11)
Range of B–O–Si angles	135.3(2)–142.9(2)	135.0(3)–143.0(3)	134.0(3)–143.0(3)	133.9(2)–142.4(2)	139.4(5)
Mean B–O–Si	138.6(2)	138.7(3)	138.5(3)	137.8(2)	139.4(5)
Range of O–Si–O angles	107.53(11)–110.51(11)	107.90(17)–110.05(17)	108.12(14)–110.32(15)	107.31(13)–110.90(13)	109.14(15)
Mean O–Si–O	109.18(11)	109.19(17)	109.03(15)	109.08(13)	109.14(15)
Range of O–B–O angles	120.9(3)–121.5(3)	120.6(4)–121.4(4)	121.0(4)–122.2(4)	120.7(3)–121.1(3)	120.6(8)
Mean O–B–O	121.1(3)	121.0(4)	121.8(4)	120.9(6)	120.6(8)
Range of O–B–C angles	118.0(3)–120.4(3)	118.8(4)–120.2(4)	117.7(4)–120.1(4)	118.8(3)–120.1(3)	119.7.(4)
Mean O–B–C	119.4(3)	119.5(4)	119.0(4)	119.5 (3)	119.7.(4)

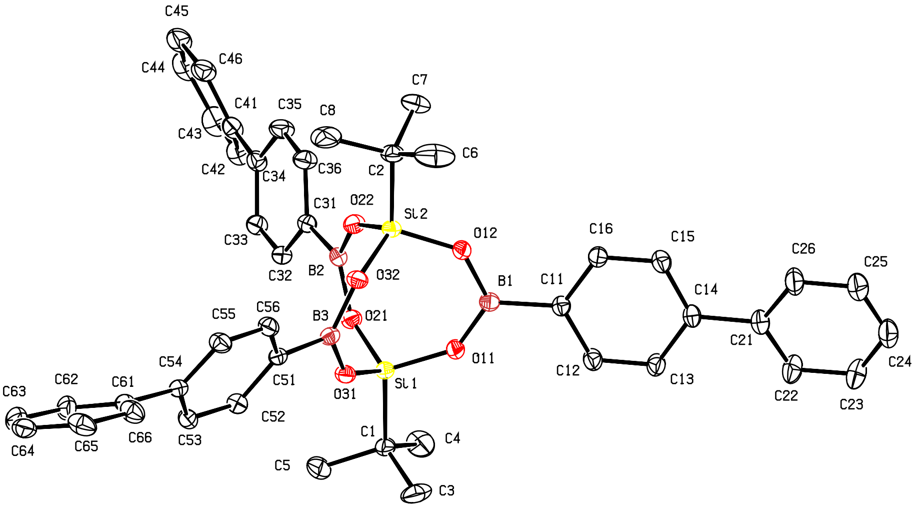

Fig. 1. An ORTEP view of $[\mathrm{Bu}^t\mathrm{Si\{O(4\text{-}PhC_6H_4B)O\}_3SiBu}^t]$ (**2**) with atom numbering.

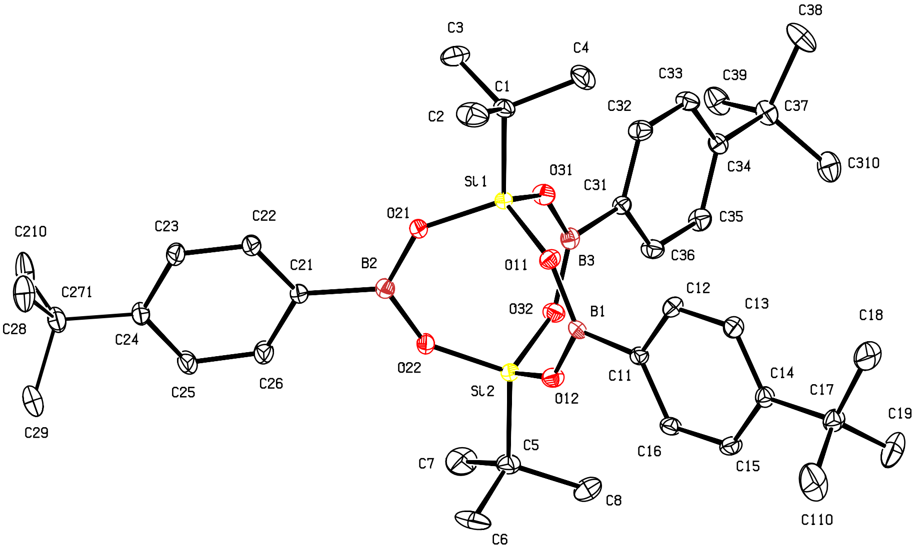

Fig. 2. An ORTEP view of $[\mathrm{Bu}^t\mathrm{Si\{O(4\text{-}Bu}^t\mathrm{C_6H_4B)O\}_3SiBu}^t]$ (**3**), with atom numbering.

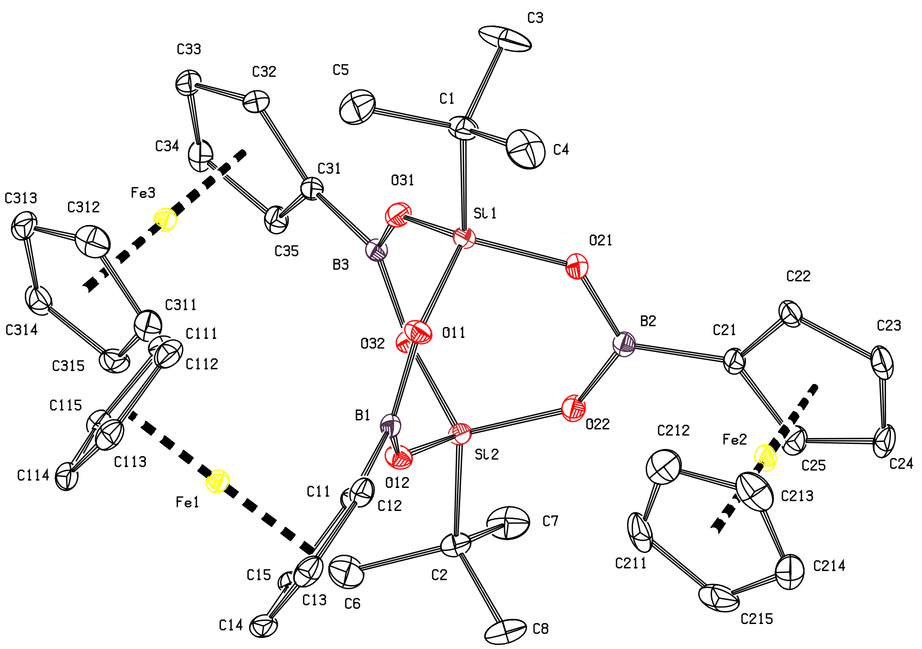

Fig. 3. An ORTEP view of [Bu^{t}Si{O(CpFeC$_5$H$_4$B)O}$_3$SiBu^t] (**6**), with atom numbering.

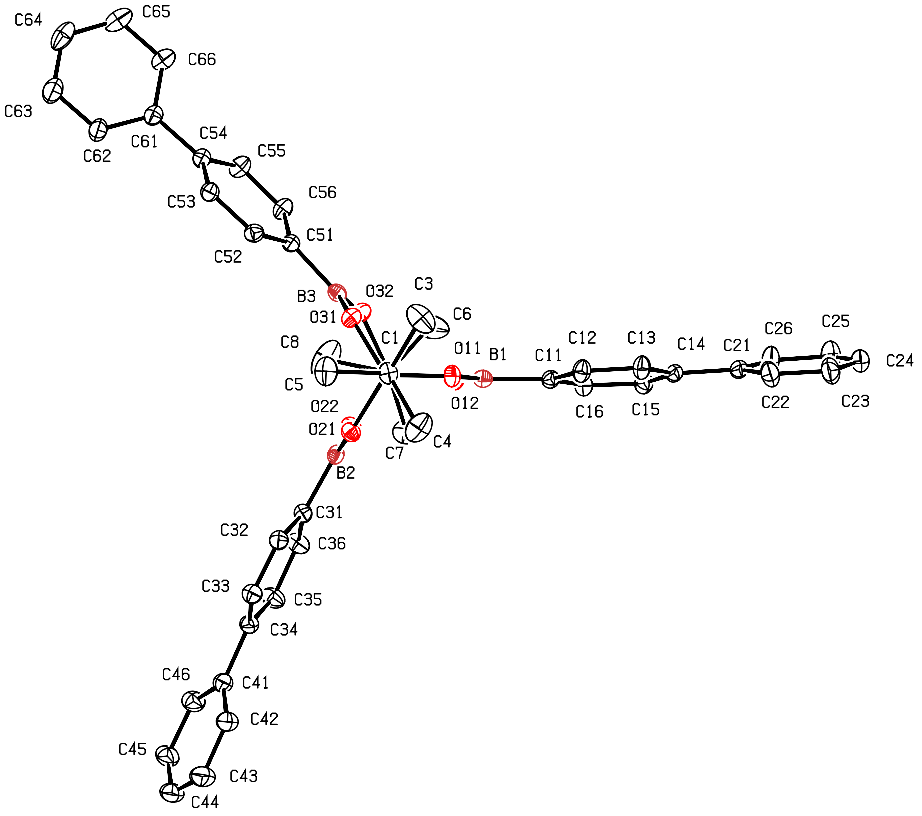

Fig. 4. ORTEP view of [Bu^{t}Si{O(4-PhC$_6$H$_4$B)O}$_3$SiBu^t] (**2**) along the Si···Si axis.

1.364(11)–1.372(10) Å and in the cube-based structure [(Bu^{t}Si)$_4$(CH$_2$=CHC$_6$H$_4$B)$_4$O$_{10}$] [6] (1.361(4)–1.369(4) Å). A mean value of 1.367 Å has been reported for B–O distances where the boron is tricoordinated [10] and the mean values of the B–O distances reported here are all the same within one s.u.

The Si–O distances in **2**, **3**, **4**, **6** and **9** vary between 1.603(3) and 1.638(3) Å, but the mean values of the six Si–O distances are remarkably similar at about 1.620 Å, Table 1. The range of previously reported Si–O distances for borosiloxanes containing trigonal boron was 1.603(2) [7] to 1.655(5) [4,11]. The mean values of Si–O distances

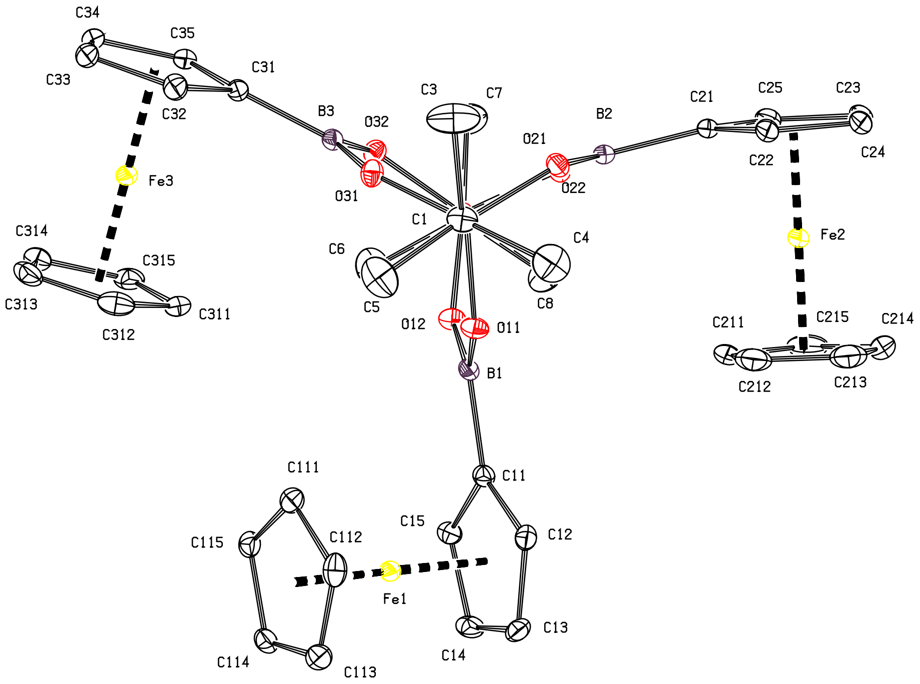

Fig. 5. ORTEP view of [Bu^{t}Si{O(CpFeC$_5$H$_4$B)O}$_3$SiBu^t] (**6**) along the Si···Si axis.

in [B(OSiPh$_2$SiPh$_2$O)$_3$B] (**14**) [5], [Bu^{t}Si{O(4-BrC$_6$H$_4$B)O}$_3$-SiBu^t] (**15**) [4] and [(Bu^{t}Si)$_4$(CH$_2$=CHC$_6$H$_4$B)$_4$O$_{10}$] [6], were 1.631(2), 1.621(5) and 1.616(4) Å, respectively, and a mean value of 1.631(2) Å has been reported for Si–O distances where the silicon is four coordinated [10].

The mean B–C distances in **2**, **3**, **4**, **6** and **9** range from 1.541(5) to 1.559(6) Å. The B–C$_{Ph}$ distances in PhB(O-SiPh$_3$)$_2$, **16** [12] and (PhBO)$_2$(OSiPh$_2$)$_2$ (**17**) [13], were 1.558(8) and 1.555(6) Å, respectively, and the B–C distances reported in [Bu^{t}Si{O(4-BrC$_6$H$_4$B)O}$_3$SiBu^t] (**15**) [4] ranged from 1.541(11) to 1.585(11) Å, with a mean value of 1.566 Å.

The average value of the Si–C distances in **2**, **3**, **4**, **6** and **9** were 1.833(3), 1.841(5), 1.829(4), 1.853(4) and 1.846(9) Å, respectively. A mean value of 1.863 Å has been reported for Si–C bonds, where C is sp^3-hybridised and bonded to carbon or hydrogen atoms only and the silicon atom is four coordinated [10].

B–O–Si angles at trigonal boron atoms are known to be very flexible [12] in both acyclic and cyclic compounds. Examples include the two chemically equivalent B–O–Si angles in PhB(OSiPh$_3$)$_2$ (**18**), {139.8(4)° and 157.9(3)°} [12], and in cyclic systems, 128.89(14)° in (PhBO)(Ph$_2$SiO)$_2$ (**19**) [14] and 160.9(3)° in (PhBO)$_2$(Ph$_2$SiO)$_2$ (**17**) [13]. Hence, it is noteworthy that in the compounds **2**, **3**, **4** and **6** the variation is relatively small at ca. ±4° from a mean angle of ca. 138°, Table 1. The six B–O–Si angles in **2** vary from 135.3(2)° to 142.9(2)° with a mean value of 138.6(2)° and those in **3** show an almost identical range of 135.0(3)–143.0(3)° and a mean value of 138.8(3)°. In **4** these angles vary from 134.0(3)° to 143.0(3)° with a mean value of 138.5(3)°. The B–O–Si angles in **6** range from 133.9(3)° to 142.4(3)° with a mean value of 137.8(9)°. Compound **9** has a symmetry determined single B–O–Si angle of 139.5(4)°. All B–O–Si angles for **2**, **3**, **4**, **6** and **9** are notably similar to those for [B(OSiPh$_2$SiPh$_2$O)$_3$B] (**14**) [5], and [Bu^t-Si{O(4-BrC$_6$H$_4$B)O}$_3$SiBu^t] (**15**) [4] where the B–O–Si angles varied over the range 137.89(18)–140.03(18)° with a mean value of 138.6(18)° for **14** and 137.5(6)–140.7(6)° with a mean value of 138.6(6)° for **15**, respectively. In the more open structure of the cube-based [(Bu^t-Si)$_4$(CH$_2$=CHC$_6$H$_4$B)$_4$O$_{10}$] [6], the B–O–Si angles vary more from 137.5(2)° to 154.4(2)°.

Like the B–O–Si angles, the O–B–O angles in **2**, **3**, **4**, **6** and **9** are notably similar and close to 121°, Table 1. The three O–B–O angles in [Bu^{t}Si{O(4-BrC$_6$H$_4$B)O}$_3$SiBu^t] (**15**) [4] varied from 119.9(8)° to 124.0(8)° the mean value being 122.2(8)° and the four O–B–O angles in [(Bu^t-Si)$_4$(CH$_2$=CHC$_6$H$_4$B)$_4$O$_{10}$] [6], varied from 120.7(3)° to 120.9(3)° with a mean value of 120.8(3)°.

The O–Si–O and O–B–C angles in **2**, **3**, **4**, **6** and **9** are even more remarkably similar with ranges and means which are almost identical, Table 1. The range over all the compounds for O–Si–O angles is from 107.29(15)° to 110.90(15)° both of which were observed in [Bu^{t}Si{O(Cp-FeC$_5$H$_4$B)O}$_3$SiBu^t] (**6**). The mean value of O–Si–O angles in **2**, **3**, **4**, **6** and **9** was 109.12° which was very close to the mean value observed in [(Bu^{t}Si)$_4$(CH$_2$=CHC$_6$H$_4$B)$_4$O$_{10}$] [6]. For [B(OSiPh$_2$SiPh$_2$O)$_3$B] (**14**) [5], the three O–Si–O angles ranged from 108.78(12)° to 109.34(10)° with a mean value of 109.12(12)°. In [Bu^tSi{O(4-BrC_6H_4B)O}$_3$SiBu^t] (**15**) [4] the O–Si–O angles ranged from 108.5(3)° to 109.7(3)° with a mean value of 109.2(3)°. The O–B–C angles range from 118.0(3)° to 120.4(3)° which are both found in **2**. The mean values in compounds **2**, **3**, **6** and **9** are all close to 119.5° and that in **4** is 119.1°. The O–B–C angles in compound **15** range from 116.6(9)° to 120.7(8)° with a mean of 118.9(8)°.

As with the O–Si–O angles, the O–Si–C angles are close to the tetrahedral value in all cases.

2.3. Reactions between the borosiloxane cage [Bu^tSi(OPhBO)$_3$SiBu^t] and pyridine or N,N,N′,N′-tetramethylethylenediamine

2.3.1. Synthesis and structural study of [Bu^tSi(OPhBO)$_3$SiBu^t] · NC_5H_5 (12)

The reaction between [Bu^tSi{O(PhB)O}$_3$SiBu^t] (**1**), and three equivalents of pyridine in ether at r.t. for 16 h followed by crystallisation of the solid product from dichloromethane–heptane (1:3) afforded [Bu^tSi{O(PhB)O}$_3$SiBu^t] · NC_5H_5 (**12**) in 73% yield. This compound was soluble in toluene, dichloromethane, ether and acetone at room temperature. Chemical analysis for C, H, B and N supported the formulation of **12** as a 1:1 adduct. The ^{11}B NMR spectrum of **12** showed two signals in a 2:1 ratio with one corresponding to three coordinate boron at 25.4 ppm and one associated with four coordinate boron at 0.6 ppm, respectively. Crystals of [Bu^tSi{O(PhB)O}$_3$SiBu^t] · NC_5H_5 (**12**) suitable for X-ray diffraction studies were grown by the slow evaporation of a dichloromethane–heptane solution of **12**. Fig. 6 is an ORTEP plot showing a general view of [Bu^tSi{O(PhB)O}$_3$SiBu^t] · NC_5H_5 (**12**), and the atom numbering scheme is shown in Fig. 6. Significant bond distance and bond angle data for **12** are given in Table 2. The basic $Si_2O_6B_3$ cage structure of [Bu^tSi{O(PhB)O}$_3$SiBu^t] · NC_5H_5 (**12**) is very similar to the $Si_2O_6B_3$ cage in the borosiloxanes **2**, **3**, **6** and **9** reported above. The structure of **12** also involves near-eclipsed arrangements of the *tert*-butyl groups at Si(1) with those at Si(21) and a "paddlewheel" arrangement of the three phenyl groups and the pyridine group is adopted as can be seen if the structure is viewed above the Si(1)···Si(21) axis.

The four B–O distances in [Bu^tSi{O(PhB)O}$_3$SiBu^t] · NC_5H_5 (**12**) for the tricoordinate boron atoms span a relatively wide range from 1.354(17) to 1.394(18) Å. The two B–O distances for the tetracoordinate bonded boron atom in **12** are 1.457(18) and 1.469(18) Å, Table 2. These values are similar to data from the tetrahedrally coordinated boron compounds Ph(OSiR_2R′)B{O$(CH_2)_3$N} (**20**), where the boron atom is directly bonded to two oxygen atoms, a Ph group and the nitrogen atom and R or R′ = Ph or Me. These compounds have B–O_{Si} distances of 1.439(4) [15] and 1.443(6) [16] in the Ph_2Me and PhMe_2 derivatives, respectively. The increased B–O distance at the tetrahedral boron site may be associated with the removal of any B–O π-bonding component on going from trigonal to tetrahedral coordination at boron.

The Si–O distances in **2**, **3**, **4**, **6** and **9** varied between 1.603(3) and 1.638(3) Å, with a mean value of 1.621 Å and these values are comparable with the four Si–O distances in [Bu^tSi{O(PhB)O}$_3$SiBu^t] · NC_5H_5 (**12**) which range from 1.625(9) to 1.631(9) Å where the boron atom is tricoordinate. The average value is 1.628 Å. The two Si–O distances where the boron atom is tetracoordinate are notably shorter with values of 1.585(7) and 1.594(9) Å suggesting that electron density has increased in the Si–O bond corresponding to the decrease in B–O electron density.

The B–N distance in [Bu^tSi{O(PhB)O}$_3$SiBu^t] · NC_5H_5 (**12**) was 1.655(17) Å. For simple borosiloxane Ph(OSiR_2R′)B{O$(CH_2)_3$N} species, **20**, the B–N distances are 1.639(4) [15] and 1.639(6) Å [16] in the Ph_2Me and PhMe_2 derivatives, respectively. A value of 1.556 Å has been reported for B–N distances where the boron atom is tetracoordinate [10].

The two B–C distances in **12** with the boron atom tricoordinate were 1.552(19) Å and 1.594(19) Å. Similar B–C distances in **2**, **3**, **4**, **6** and **9** with mean values of 1.553(4), 1.546(6), 1.559(6), 1.541(5) and 1.544(10) Å were noted in Table 1. A mean value of 1.556 Å has been reported for B–C_{ar} distances, where the boron atom is tricoordinate and the carbon atom is part of an aromatic system [10]. The B–C distance in **12** where the boron atom is tetracoordinate was 1.58(2) Å which is within 3x s.u. of the two other B–C distances. The mean Si–C distance in **12** was typical of such distances at 1.832(15) Å.

In [Bu^tSi{O(PhB)O}$_3$SiBu^t] · NC_5H_5 (**12**) the four B–O–Si angles in which the boron is tricoordinate range from 134.4(10)° to 140.7(9)° which is a similar range to the corresponding angles in **2**, **3**, **6** and **9**, Table 1. The two B–O–Si angles in **12** where the boron is tetracoordinate are 134.2(8)° and 138.0(9)°.

The O–B–O angles in [Bu^tSi{O(PhB)O}$_3$SiBu^t] · NC_5H_5 (**12**) vary from 111.6(11)° at the tetracoordinate boron atom to 121.1(13)° and 122.3(13)° at the tricoordinate boron atoms. These angles are close to the 109° and 120° expected for tetrahedral and trigonal planar geometries, respectively. Likewise the O–Si–O angles in **12** range from 108.2(5)° to 111.0(5)° with a mean value of 109.6(5)° which is normal for tetrahedral silicon and the four O–B–C angles in [Bu^tSi{O(PhB)O}$_3$SiBu^t] · NC_5H_5 (**12**) where the boron is trigonal planar range from 117.9(12)° to 120.1(13)°. The two O–B–C values in **12** where the boron atom is tetrahedral had values greater than 109° at 112.6(11)° and 115.5(12)°, respectively.

The six O–Si–C angles in **12** ranged from 106.4(6)° to 112.6(5)° with a mean value of 109.4(6)° but the angles where the oxygen is bonded to a tetracoordinate boron atom, mean value 112.4(6)°, appeared to be larger than the O–Si–C angles where the oxygen is bonded to a trigonal boron, mean value 107.9(6)°.

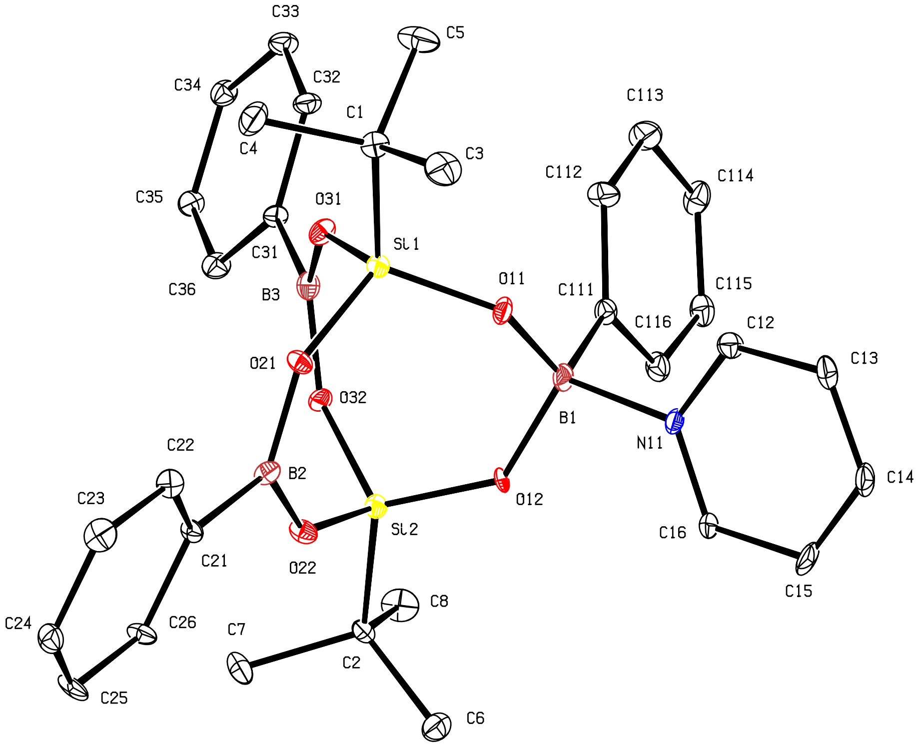

Fig. 6. An ORTEP view of $[Bu^{t}Si(OPhBO)_3SiBu^{t}] \cdot NC_5H_5$ (**12**), with atom numbering. Selected interatomic distances (Å) and angles (°): Si(1)–O(11) 1.594(9), Si(1)–O(21) 1.630(9), Si(1)–O(31) 1.631(9), Si(1)–C(1) 1.832(15), Si(2)–O(12) 1.585(7), Si(2)–O(22) 1.626(9), Si(2)–O(32) 1.625(9), Si(2)–C(2) 1.831(14), B(1)–N(11) 1.655(17), B(1)–O(11) 1.457(18), B(1)–O(12) 1.469(18), B(1)–C(111) 1.58(2), B(2)–O(21) 1.394(18), B(2)–O(22) 1.370(17), B(2)–C(21) 1.552(19), B(3)–O(31) 1.354(17), B(3)–O(32) 1.375(19), B(3)–C(31) 1.594(19); O(11)–Si(1)–O(21) 111.0(5), O(11)–Si(1)–O(31) 109.6(5), O(21)–Si(1)–O(31) 108.2(5), O(11)–Si(1)–C(1) 111.8(6), O(21)–Si(1)–C(1) 106.4(6), O(31)–Si(1)–C(1) 109.7(6), O(12)–Si(2)–O(22) 109.3(5), O(12)–Si(2)–O(32) 110.6(5), O(22)–Si(2)–O(32) 108.6(5), O(12)–Si(2)–C(2) 112.6(5), O(22)–Si(2)–C(2) 106.4(6), O(32)–Si(2)–C(2) 109.2(6), B(1)–O(11)–Si(1) 138.0(9), B(2)–O(21)–Si(1) 139.7(9), B(3)–O(31)–Si(1) 134.4(10), B(1)–O(12)–Si(2) 134.2(8), B(2)–O(21)–Si(2) 137.3(9), B(3)–O(32)–Si(2) 140.7(9), O(12)–B(1)–O(11) 111.6(11), O(11)–B(1)–C(111) 115.5(12), O(12)–B(1)–C(111) 112.6(11), O(11)–B(1)–N(11) 103.2(10), O(12)–B(1)–N(11) 104.9(11), C(111)–B(1)–N(11) 107.9(10), O(21)–B(2)–C(21) 120.1(13), O(21)–B(2)–C(22) 118.8(12), O(21)–B(2)–O(22) 121.1(13), O(31)–B(3)–O(32) 122.3(13), O(32)–B(3)–C(31) 117.9(12), O(31)–B(3)–C(31) 119.8(13).

Table 2
Summary of crystal data details for **2**, **3**, **4**, **6**, **9** and **12**

Crystal data	**2**	**3**	**4**	**6**	**9**	**12**
Empirical formula	$C_{44}H_{45}B_3O_6Si_2$	$C_{38}H_{57}B_3O_6Si_2$	$C_{29.5}H_{33.5}B_3N_3O_{12}Si_2$	$C_{38}H_{45}B_3Fe_3O_6Si_2$	$C_{26}H_{27}B_3F_6O_6Si_2$	$C_{31}H_{38}B_3NO_6Si_2$
Molar mass	758.41	698.45	710.70	853.9	638.09	609.23
Color	colourless	colourless	colourless	orange	colourless	colourless
Habit	plate	needle	block	block	cube	block
a (Å)	12.9156(17)	12.5922(16)	9.533(2)	10.4736(11)	15.6121(8)	11.030(6)
b (Å)	15.6120(9)	13.8371(18)	20.295(3)	10.9281(14)	15.6121(8)	18.227(6)
c (Å)	22.678(2)	24.674(2)	18.697(3)	19.0690(28)	15.6121(8)	16.235(5)
α (°)	90.00	90.00	90.00	97.905(11)	90.00	90.00
β (°)	103.899(9)	93.830(9)	101.775(12)	102.628(10)	90.00	94.24(3)
γ (°)	90.00	90.00	90.00	106.750(10)	90.00	90.00
V (Å^3)	4311.0(7)	4289.6(10)	3541.4(11)	1991.9(4)	3805.3(3)	3255(2)
Space group	$P2_1/c$	$P2_1/c$	$P2_1/c$	$P\bar{1}$	P_{4132}	Cc
Z	4	4	4	2	4	4
F(000)	1600	1504	1482	884	1312	1288
D_{calc} (g cm^{-1})	1.169	1.081	1.333	1.424	1.114	1.243
μ (mm^{-1})	0.127	0.122	0.164	1.182	0.153	0.152
T (K)	294(1)	294(1)	293(2)	293(2)	293(2)	150(2)
Reflections measured	8019	7964	3338	9117	657	2828
R	0.0549	0.0638	0.0739	0.0427	0.0828	0.0711
R_w	0.1085	0.1709	0.1497	0.0987	0.1391	0.1569
Goodness-of-fit	0.916	1.043	0.919	1.151	1.197	1.104

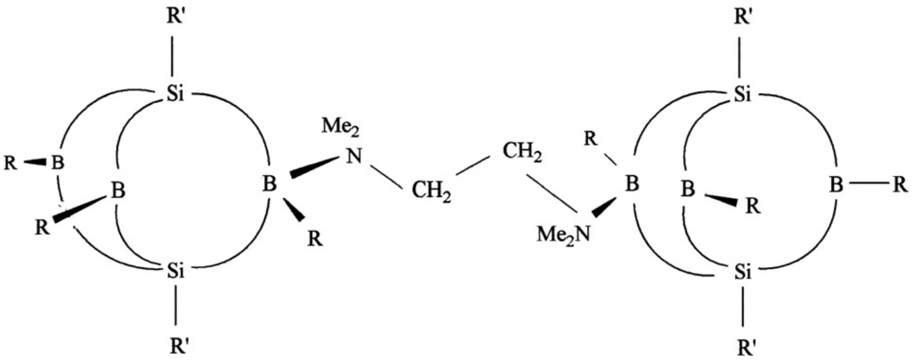

Diagram 2.

2.4. Synthesis of $[Bu^tSi\{O(PhB)O\}_3SiBu^t]_2 \cdot Me_2NCH_2CH_2NMe_2$ (**13**)

The reaction between $[Bu^tSi\{O(PhB)O\}_3SiBu^t]$ (**1**), and one equivalent of *N*,*N*,*N*′,*N*′-tetramethylethylenediamine in ether at r.t. for 8 h afforded $[Bu^tSi\{O(PhB)O\}_3SiBu^t]_2 \cdot Me_2NCH_2CH_2NMe_2$ (**13**) in low yield (27%) after crystallisation of the crude product from CH_2Cl_2–heptane (1:2) solution. As with compounds **1**–**12**, this compound was soluble in typical organic solvents such as toluene, dichloromethane, ether and acetone at room temperature. Chemical analysis for C, H, B and N suggested the formulation of **13** as a 2:1 adduct and FT-IR and multinuclear NMR spectroscopy supported this formulation. The ^{11}B NMR spectrum showed signals at 31.8 and 2.8 ppm in a ratio of 2:1 which correspond to three and four coordinate boron environments, respectively. On the basis of these data we suggest that the overall structure of **13** is as shown in Diagram 2.

Unfortunately, crystals suitable for an X-ray diffraction study could not be obtained even after many attempts from many different solvents.

3. Conclusions

Eleven borosiloxane $[R'Si(ORBO)_3SiR']$ cage compounds ($R' = Bu^t$ and R = Ph (**1**), $4\text{-}PhC_6H_4$ (**2**), $4\text{-}Bu^tC_6H_4$ (**3**), $3\text{-}NO_2C_6H_4$ (**4**), $4\text{-}CH(O)C_6H_4$ (**5**), $CpFeC_5H_4$ (**6**), $4\text{-}C(O)CH_3C_6H_4$ (**7**), $4\text{-}ClC_6H_4$ (**8**) and $R = 2,4\text{-}F_2C_6H_3$ (**9**), and $R' =$ *cyclo*-C_6H_{11} and R = Ph (**10**) and $4\text{-}BrC_6H_4$ (**11**)) have been synthesized and characterized by spectroscopic (IR, NMR), mass spectrometric and for compounds where $R' = Bu^t$ and $R = 4\text{-}PhC_6H_4$ (**2**), $4\text{-}Bu^tC_6H_4$ (**3**), $3\text{-}NO_2C_6H_4$ (**4**), $CpFeC_5H_4$ (**6**) and $2,4\text{-}F_2C_6H_3$ (**9**) X-ray diffraction studies. These compounds contain trigonal planar RBO_2 and tetrahedral $R'SiO_3$ units located around 11-atom "spherical" $B_3Si_2O_6$ cores. The reaction between $[Bu^tSi\{O(PhB)O\}_3SiBu^t]$, **1**, and excess pyridine yields a 1:1 adduct while the reaction between **1** and *N*,*N*,*N*′,*N*′-tetramethylethylenediamine in equimolar amounts affords a 2:1 borosiloxane:amine adduct.

It is clear from the structural analyses of 2, 3, 4, 6 and 9 that the $B_3Si_2O_6$ core structures are very similar and those in 2 and 3 being almost identical. All the structures involve near eclipsed arrangements of the *tert*-butyl groups at Si(1) and Si(2) when viewed along the Si···Si axis. The B–O–Si angles in the $B_3Si_2O_6$ cores of 2, 3, 4, 6 and 9 are found in a relatively narrow range from 134.0° to 143.0°. The structure of the pyridine adduct, 12, was determined with X-ray techniques. It had two trigonal planar RBO_2 units and one tetrahedral RBO_2N unit and a number of features in common with the unadducted compounds including a narrow range of B–O–Si angles (133.2–140.9°).

4. Experimental

All reactions were carried out under an inert atmosphere of dry nitrogen. Solvents were dried and distilled prior to use. Both *tert*-butylsilanetriol and *cyclo*-hexylsilanetriol were prepared according to the literature synthesis of $Bu^tSi(OH)_3$ [17]. All boronic acids used were obtained from either Aldrich or Lancaster Chemical Co. and used as supplied. Infrared spectra were recorded as KBr disks on a Perkin–Elmer Paragon 1000 FT-IR Spectrometer. ^1H and ^{13}C NMR spectra were recorded in $CDCl_3$ solvent on a JEOL FT NMR Spectrometer, GSX-270 Series or, for ^{11}B and ^{29}Si NMR spectra, on a Bruker AM 400. Chemical shifts δ are expressed in ppm relative to $\Xi = 100$ MHz for δ (^1H) (quoted ±0.05 ppm) (standard $SiMe_4$) and $\Xi = 32.083971$ MHz for δ (^{11}B) (quoted ±0.5 ppm) (nominally F_3BOEt_2 in $CDCl_3$). Mass spectra (EI, 70 eV) were recorded on a Kratos Profile GC–MS Spectrometer. Elemental analyses were carried out on a Perkin–Elmer 240C elemental analyser at the Microanalytical Laboratory, University College, Cork.

4.1. Syntheses of borosiloxane $[R^1Si(ORBO)_3SiR^1]$ cage compounds ($R^1 = Bu^t$ and R = Ph (**1**); $4\text{-}PhC_6H_4$ (**2**); $4\text{-}Bu^tC_6H_4$ (**3**); $3\text{-}NO_2C_6H_4$ (**4**); $4\text{-}CH(O)C_6H_4$ (**5**); $CpFeC_5H_4$ (**6**); $4\text{-}C(O)CH_3C_6H_4$ (**7**); $4\text{-}ClC_6H_4$ (**8**); $2,4\text{-}F_2C_6H_3$ (**9**); and $R^1 =$ cyclo-C_6H_{11} and R = Ph (**10**); $4\text{-}BrC_6H_4$ (**11**))

4.1.1. Synthesis of $[Bu^tSi\{O(PhB)O\}_3SiBu^t]$ (**1**)

A mixture of *tert*-butylsilanetriol (0.507 g, 3.72 mmol) and phenylboronic acid (0.680 g, 5.58 mmol) in toluene

(50 ml) was heated at reflux temperature in a Dean-Stark apparatus for 10 h. After cooling, the removal of toluene on a rotary evaporator (40 °C) yielded a colourless solid. This was crystallised from hot benzene (50°C) affording [Bu^{t}Si{O(PhB)O}$_3$SiBu^t] (153, 0.943 g, 95.7%), m.p. 220–222°C. *Anal.* Calc. for $C_{26}H_{33}B_3O_6Si_2$: C, 58.9; H, 6.3; B, 6.1. Found: C, 59.05; H, 6.2; B, 6.0%. FT-IR (KBr) ν_{max}/cm^{-1}: 1305(vs), 1133(vs), 677(s). ^{1}H NMR (CDCl$_3$, 294 K): δ: 7.91–7.22 [m, 5H, C_6H_5]; 1.35 [s, 6H, C(CH_3)$_3$]. ^{13}C NMR (CDCl$_3$, 294 K) δ: 135.5, 133.4, 132.2, 127.9 [all C_6H$_5$]; 25.5 [C(CH$_3$)$_3$]; 16.6 [C(CH$_3$)$_3$]. MS, *m*/*z*: 530 [M]$^+$, 473 [M−Bu]$^+$, 453 [M−Ph]$^+$.

4.1.2. Synthesis of [Bu^{t}Si{O(4-$C_6H_5C_6H_4$)BO}$_3$SiBu^t (2)

The procedure was the same as that described for **1**. The quantities used were: *tert*-butylsilanetriol (0.1536g, 1.13 mmol); 4-biphenylboronic acid (0.3254g, 1.64 mmol); toluene 50ml; reaction time 18 h. Crystallisation from CH$_2$Cl$_2$–heptane (1:3) afforded [Bu^{t}Si{O(4-$C_6H_5C_6H_4$)-BO}$_3$SiBu^t], **2** (0.35 g, 81.1%), mp 282–284 °C. *Anal.* Calc. for $C_{44}H_{45}O_6B_3Si_2$: C, 69.7; H, 6.3. Found: C, 69.6; H, 6.3%. FT-IR (KBr) ν_{max}/cm^{-1}: 1299(vs), 1132(vs), 660(s). ^{1}H NMR (CDCl$_3$, 294 K): δ 8.03–7.21 [m, 3H, $C_6H_4C_6H_5$], 1.33 [s, 2H, C(CH_3)$_3$], ^{11}B NMR (CDCl$_3$, 294 K) δ 28.3, ^{13}C NMR (CDCl$_3$,294 K) δ 144.4, 141.0, 135.9, 131.0, 127.9, 126.8, 126.5 [all C_6H$_4$$C_6H_5$], 26.6 [C($CH_3$)$_3$], 16.3 [$C$(CH$_3$)$_3$], ^{29}Si NMR (CDCl$_3$, 294 K) δ −57.5. Crystal data for **2**, see Table 1.

4.1.3. Synthesis of [Bu^{t}Si{O(4-Bu^tC_6H_4)BO}$_3$SiBu^t] (3)

The procedure was the same as that described for **1**. The quantities used were: *tert*-butylsilanetriol (0.1311 g, 0.96 mmol); *tert*-butylphenylboronic acid (0.2548 g, 1.43 mmol); toluene 50 ml; reaction time 15 h. Crystallisation from CH$_2$Cl$_2$–heptane (1:2) afforded [Bu^{t}Si{O-(4Bu^tC_6H_4)BO}$_3$SiBu^t] (**3**) (0.24 g, 74.9%). mp 253–255 °C. Found: C, 65.3; H, 8.2. *Anal.* Calc. for $C_{38}H_{57}O_6B_3Si_2$: C, 65.3; H, 8.2. Found: C, 65.3; H, 8.2. FT-IR (KBr) ν_{max}/cm^{-1}: 1302(vs), 1137(s), 660(m). MS, *m*/*z*: 698 [M]$^+$, 641 [M−Bu]$^+$, 57 [Bu]$^+$. Crystal data for **3**: see Table 1.

4.1.4. Synthesis of [Bu^{t}Si{O(3-NO$_2$$C_6H_4$)BO}$_3$SiBu^t] (4)

The procedure was the same as that described for **1**. The quantities used were: *tert*-butylsilanetriol (0.430 g, 3.16 mmol), 3-nitrophenylboronic acid (0.789 g, 4.73 mmol), toluene, 50ml; reaction time 10 h. The product, [Bu^{t}Si{OB(3-$C_6H_4NO_2$)O}$_3$SiBu^t] · (0.5C_7H_8), crystallised from a toluene solution at room temperature. Yield 0.913 g (87.1%) of **4**, m.p. 176–178°C. Found: C, 49.9; H, 4.9; N, 5.8; B, 4.3%. *Anal.* Calc. for $C_{29.5}H_{34}B_3N_3O_{12}Si_2$: C, 49.8; H, 4.8; N, 5.9; B, 4.6. Found: C, 49.9; H, 4.9; N, 5.8; B, 4.3%. FT-IR (KBr) ν_{max}/cm^{-1}: 1300(vs), 1143(vs), 657(m). ^{1}H NMR (CDCl$_3$, 294 K): δ: 8.67–7.31 [m, 2H, C$_6$$H_4NO_2$]; 1.43 [s, 3H, C(C$H_3$)$_3$]. ^{13}C NMR (CDCl$_3$, 294 K) δ: 148.4, 141.4, 134.2, 130.0, 128.7, 127.1 [all C_6H$_4$NO$_2$]; 25.7 [C(CH$_3$)$_3$]; 16.6 [C(CH$_3$)$_3$]. MS, *m*/*z*: 665 [M]$^+$, 619 [M−NO$_2$]$^+$, 608 [M−Bu]$^+$, 451 [M−2NO$_2$–$C_6H_4NO_2$]$^+$, 122 [$C_6H_4NO_2$]$^+$, 57 [Bu]$^+$.

4.1.5. Synthesis of [Bu^{t}Si{O(4-CHOC_6H_4)BO}$_3$SiBu^t] (5)

The procedure was the same as that described for **1**. The following quantities were used: *tert*-butylsilanetriol (0.4021 g, 2.96 mmol); 4-formylphenylboronic acid (0.6621 g, 4.41 mmol); toluene, 50 ml; reaction time 18 h. This afforded [Bu^{t}Si{O(4-CHOC_6H_4)BO}$_3$SiBu^t] (**5**) as a colourless crystalline solid (0.75 g, 82.1%), mp 194–196 °C. *Anal.* Calc. for $C_{29}H_{33}O_9B_3Si_2$: C, 56.7; H, 5.4. Found: C, 56.5; H, 5.6%. FT-IR (KBr) ν_{max}/cm^{-1}: 1298(vs), 1128(vs), 681(s). ^{1}H NMR (CDCl$_3$, 294 K): δ 9.98 [s, 3H, C$_6$H$_4$CHO], 8.00–7.19 [m, 4H, C$_6$$H_4$CHO], 1.27 [s, 6H, C(C$H_3$)$_3$], ^{13}C NMR (CDCl$_3$, 294 K): δ 192.4 [C$_6H_4$$C$HO], 138.7, 135.8, 128.9 [all C_6H$_4$CHO], 25.8C(CH$_3$)$_3$], 16.2 [C(CH$_3$)$_3$]. MS, *m*/*z*: 614 [M]$^+$, 105 [C$_6$H$_4$CHO]$^+$, 57 [Bu]$^+$.

4.1.6. Synthesis of [Bu^{t}Si{O(CpFeC_5H_4)BO}$_3$SiBu^t] (6)

The procedure was the same as that described for **1**. The following quantities were used: *tert*-butylsilanetriol (0.1971 g, 1.45 mmol); ferrocenylboronic acid (0.5211 g, 2.25 mmol); toluene, 60 ml; reaction time 15 h. Crystallisation from CH$_2$Cl$_2$–heptane (1:3) afforded orange crystals of [Bu^{t}Si(OC$_5$H$_4$FeCpBO)$_3$SiBu^t] (**6**) (0.50 g, 82.2%), m.p. 244–246 °C. *Anal.* Calc. for $C_{38}H_{45}O_6B_3Fe_3Si_2$: C, 53.4; H, 5.3. Found: C, 53.4; H, 5.3%. FT-IR (KBr) ν_{max}/cm^{-1}: 1316(s), 1290(s), 621(m). MS, *m*/*z*: 854 [M]$^+$, 186 [(C$_5$H$_5$FeC$_5$H$_5$)]$^+$. Crystal data for **6**: see Table 1.

4.1.7. Synthesis of [Bu^{t}Si{O(CH$_3$C(O)C_6H_4B)O}$_3$SiBu^t] (7)

The procedure was the same as that described for **1**. The following quantities were used: *tert*-butylsilanetriol (0.3024 g, 2.22 mmol); 4-acetylphenylboronic acid (0.5511 g, 3.31 mmol); toluene, 50 ml; reaction time 18 h. This afforded [Bu^{t}Si{O(CH$_3$C(O)C$_6$H$_4$B)O}$_3$SiBu^t] (**7**) as a crystalline solid (0.54 g, 75.2%), m.p. 134–135 °C. *Anal.* Calc. for $C_{32}H_{39}O_9B_3Si_2$: C, 58.5; H, 6.0. Found: C, 58.6; H, 6.1%. FT-IR (KBr) ν_{max}/cm^{-1}: 1301(vs), 1133(s), 632(m). ^{1}H NMR (CDCl$_3$, 294 K): δ 8.04–7.26 [m, 4H, C$_6$$H_4$]; 2.62 [s, 3H, C(O)C$H_3$]; 1.27 [s, 6H, C(C$H_3$)$_3$]. ^{13}C NMR (CDCl$_3$, 294 K): δ 198.1 [C(O)CH$_3$]; 139.8, 137.2, 135.9, 134.1, 127.9 [all C_6H$_4$]; 27.0 [C(O)CH$_3$]; 25.5 [C(CH$_3$)$_3$], 16.3 [C(CH$_3$)$_3$]. MS, *m*/*z*: 656 [M]$^+$, 599 [M−Bu]$^+$, 57 [Bu]$^+$.

4.1.8. Synthesis of [Bu^{t}Si{O(4-ClC_6H_4)BO}$_3$SiBu^t] (8)

The procedure was the same as that described for **1**. The quantities of starting materials used were: *tert*-butylsilanetriol (0.1541 g, 1.13 mmol); 4-chlorophenylboronic acid (0.2641 g, 1.67 mmol); toluene 60 ml; reaction time 16 h. Crystallisation from a toluene–heptane (ca. 1:3) solution afforded [Bu^{t}Si{O(4-ClC_6H_4)BO}$_3$SiBu^t] (**8**) (0.29 g, 34.1%), m.p. 304–308 °C. *Anal.* Calc. for $C_{26}H_{30}O_6B_3Cl_3Si_2$: C, 49.4; H, 4.7. Found: C, 49.6; H, 4.5%.

FT-IR (KBr) ν_{max}/cm^{-1}: 1306(vs), 1130(m), 678(m). ^{1}H NMR (CDCl$_3$, 294 K): δ 7.81–7.20 [m, 2H, C_6H_4Cl];. 1.26 [s, 3H, $C(CH_3)_3$]. (HR-MS), *m*/*z*: Found 632.094. Calculated for $^{12}C_{26}{}^{1}H_{30}{}^{11}B_3{}^{35}Cl_3{}^{6}O_6{}^{28}Si_2$ 632.017.

4.1.9. *Synthesis of* $[Bu^tSi\{O(2,4\text{-}F_2C_6H_3)BO\}_3SiBu^t]$ *(**9**)*

The procedure was the same as that described for **1**. The following quantities were used: *tert*-butylsilanetriol (0.4112 g, 3.0 mmol); 2,6 difluorophenylboronic acid (0.6821 g, 4.4 mmol); toluene, 60 ml; reaction time 15 h. Crystallisation from CH_2Cl_2–heptane (1:3) afforded $[Bu^tSi\{O(2,4\text{-}F_2C_6H_3)BO\}_3SiBu^t]$ (**9**) (0.75 g, 87.3%), m.p. 183–185°C. *Anal.* Calc. for $C_{36}H_{27}B_3F_6O_6Si_2$: C, 49.0; H, 4.3. Found: C, 50.1H, 4.4%. FT-IR (KBr), ν_{max}/cm^{-1}: 1310(s), 1130(vs), 651(m). ^{1}H NMR (CDCl$_3$, 294 K): δ 7.80–6.75[m, 1H, C_6H_3], 1.26[s, 2H, $C(CH_3)_3$]. ^{29}Si NMR (CDCl$_3$, 294 K) δ −58.12. Crystal data for **9**, see Table 2.

4.1.10. *Synthesis of* $[C_6H_{11}Si\{O(PhB)O\}_3SiC_6H_{11}]$ *(**10**)*

The procedure was essentially the same as that described for **1**. The quantities used were: *cyclo*hexylsilanetriol (0.4162 g, 2.54 mmol); phenylboronic acid (0.4599 g, 3.77 mmol); toluene 50 ml; reaction time 14 h. Crystallisation from CH_2Cl_2, toluene and heptane (1:1:2) afforded $[C_6H_{11}Si\{O(PhB)O\}_3SiC_6H_{11}]$ (**10**) (0.30 g, 42.2%), m.p. 192–194 °C. *Anal.* Calc. for $C_{30}H_{37}O_6B_3Si_2$: C, 61.8; H, 6.4. Found: C, 62.1; H, 6.3%. FT-IR (KBr), ν_{max}/cm^{-1}: 1306(vs), 1140(vs), 639(s). ^{1}H NMR (CDCl$_3$, 294 K): δ 7.53–7.17 [m, 15H, C_6H_5]; 2.12–1.12 [m, 22H, C_6H_{11}].

4.2. *Synthesis of* $[C_6H_{11}Si\{O(4\text{-}BrC_6H_4B)O\}_3SiC_6H_{11}]$ *(**11**)*

The procedure was essentially the same as that described for **1**. The quantities of reagents were: *cyclo*hexylsilanetriol (0.3199 g, 1.97 mmol), bromophenylboronic acid (0.7011 g, 3.49 mmol); toluene 50 ml; reaction time 10 h. A benzene solution was layered with *cyclo*hexane (ca. 1:3). The microcrystalline product was $[C_6H_{11}Si\{O(4\text{-}BrC_6H_4B)O\}_3SiC_6H_{11}]$ (**11**) (0.44 g, 57.3%), m.p. 252–254 °C. *Anal.* Calc. for $C_{30}H_{34}O_6B_3Br_3Si_2$: C, 44.0; H, 4.2; Br, 29.3. Found: C, 44.0; H, 4.3; Br, 29.4%. FT-IR (KBr), ν_{max}/cm^{-1}: 1300(vs), 1129(vs), 636(s). ^{1}H NMR (CDCl$_3$, 294 K): δ 7.90–7.25[m, 6H, C_6H_4Br]; 2.17–2.13 [m, 11H, C_6H_{11}].

4.3. *Reactions between* $[Bu^tSi\{O(PhB)O\}_3SiBu^t]$ *(**1**) and (a) pyridine, (b) N,N,N′,N′-tetramethylethylenediamine*

4.3.1. *Synthesis of* $[Bu^tSi\{O(PhB)O\}_3SiBu^t]\cdot C_5H_5N$ *(**12**)*

Compound **1**, $[Bu^tSi\{O(PhB)O\}_3SiBu^t]$ (0.11 g, 0.275 mmol) was dissolved in ether (30 ml). While vigorously stirring, pyridine (0.05 g, 6.23 mmol) was added via micopipette. The reaction mixture was stirred for 16 h. Removal of ether on a rotary evaporator afforded a colourless product. Crystallisation from CH_2Cl_2–heptane (1:3) yielded $[Bu^tSi\{O(PhB)O\}_3SiBu^t]\cdot C_5H_5N$ (**12**) (0.046 g, 73.4%), m.p. 218–219 °C. *Anal.* Calc. for $C_{31}H_{38}O_6B_3NSi_2$: C, 61.1; H, 6.2; N, 2.3; B, 5.4. Found: C, 61.7; H, 6.3; N, 2.9; B, 5.1%. FT-IR (KBr) ν_{max}/cm^{-1}: 1327(s), 1297(s), 1194(s), 1103(s), 1051(s), 1018(s), 701(s). ^{1}H NMR (CDCl$_3$, 294 K): δ 8.80–7.21 [m, 10H, C_6H_5 and C_5H_5], 1.32 [s, 9H, $C(CH_3)_3$]. ^{13}C NMR (CDCl$_3$, 294 K): δ 147.3, 137.7, 134.3, 130.0, 127.4, 124.3 [all C_6H_5 and C_5H_5], 25.6 [$C(CH_3)_3$], 16.6 [$C(CH_3)_3$]. ^{11}B NMR (CDCl$_3$, 294 K): δ 25.5 OB(Ph)O, 0.6 OPhBO(NC_5H_5). Crystal data for **12**: see Table 2.

4.3.2. *Synthesis of* $[Bu^tSi\{O(PhB)O\}_3SiBu^t]_2\cdot Me_2NCH_2CH_2NMe_2$ *(**13**)*

Compound **1** (0.251 g, 0.473 mmol) was dissolved in ether (40 ml). *N*,*N*,*N*′,*N*′-Tetramethylethylenediamine (0.055 g, 0.472 mmol) was added via micropipette and a colourless precipitate formed. With further stirring, this almost completely dissolved. After 8 h, the solution was filtered. Removal of the solvent gave a colourless powder. Crystallisation from CH_2Cl_2–heptane (1:2) afforded $[Bu^tSi\{O(PhB)O\}_3SiBu^t]_2\cdot Me_2NCH_2CH_2NMe_2$ (**13**) (0.151 g, 27.3%), m.p. 233–234 °C. *Anal.* Calc. for $C_{58}H_{82}O_{12}B_6N_2Si_4$:C, 59.2; H, 7.0, N, 2.4; B, 5.6. Found: C, 58.8; H, 6.9; N, 2.2; B, 5.4%. FT-IR (KBr) ν_{max}/cm^{-1}: 1439(s), 1356(s), 1308(vs), 1165(s), 1172(s), 1085(s), 1032(s), 680(s), 652(s). ^{1}H NMR (CDCl$_3$, 294 K): δ 7.81–7.14 [m, 15H, C_6H_5]; 2.62 [m, 2H, $Me_2NCH_2CH_2NMe_2$], 2.21 [s, 6H, $(CH_3)_2NCH_2\text{-}CH_2N(CH_3)_2$], 1.34 [s, 18H, $C(CH_3)_3$], ^{13}C NMR (CDCl$_3$, 294 K): δ 135.5, 134.9, 131.2, 129.7, 127.4 [all, C_6H_5], 55.4 [$Me_2NCH_2CH_2NMe_2$], 44.9[$(CH_3)_2NCH_2\text{-}CH_2N(CH_3)_2$], 26.1 [$C(CH_3)_3$], 16.3 [$C(CH_3)_3$]. ^{11}B NMR (CDCl$_3$, 294 K): δ 31.8 OB(Ph)O and 2.8 OPhBO(Me_2NCH_2)$_2$.

4.3.3. *Data Collection and structure refinement for compounds **2**, **3**, **4**, **6**, **9** and **12***

Data for **2**, **3** and **4** were collected on an Enraf-Nonius CAD-4 diffractometer with graphite-monochromatised Mo Kα radiation ($\lambda = 0.71073$ Å). Data for **6**, **9** and **12** were collected on a Nonius MACH3 diffractometer with graphite-monochromatised Mo Kα radiation ($\lambda = 0.71073$ Å). Data analysis for **2**, **3**, **4** [18], **6**, **9** and **12** [19] were carried out to provide 8018, 7964, 7780, 9117, 3379 and 5384 independent reflections, respectively. The structures were solved using direct methods [20]. Non-hydrogen atoms were refined with anisotropic thermal parameters. The hydrogen atoms bonded to carbon were included in geometric positions and given thermal parameters equivalent to 1.2 times those of the atom to which they were attached, although a 1.5 factor was used for the methyl groups. A Gaussian absorption correction on **2** was carried out [18]. For **9** there was disordered solvent present which could not be modelled correctly and was removed using the SQUEEZE algorithm [21].

The structures were refined on F^2 [22] to R$_1$ 0.055, 0.064, 0.074, 0.043, 0.083 and 0.071 for 3389, 3115, 3338, 6403, 496 and 1589 reflections, respectively, with $I > 2\sigma(I)$ and

wR_2 0.127, 0.193, 0.177, 0.129, 0.155 and 0.238 for all independent reflections.

Acknowledgements

The ^{11}B and ^{29}Si NMR spectra were kindly recorded on a Bruker AM 400 instrument at the University of Leeds by Prof. J.D. Kennedy. G.F. and S.E.L. thank NSERC Canada and University College Cork for funds for diffractometers.

Appendix A. Supplementary material

CCDC 615803, 615804, 615805, 615806, 615807 and 615808 contain the supplementary crystallographic data for this paper. These data can be obtained free of charge via http://www.ccdc.cam.ac.uk/conts/retrieving.html, or from the Cambridge Crystallographic Data Centre, 12 Union Road, Cambridge CB2 1EZ, UK; fax: (+44) 1223-336-033; or e-mail: deposit@ccdc.cam.ac.uk. Supplementary data associated with this article can be found, in the online version, at doi:10.1016/j.poly.2006.12.045.

References

[1] F.J. Feher, T.A. Budzichowski, Polyhedron 14 (1995) 3239, and references therein.

[2] S.S. Kumar, H.W. Roesky, Dalton Trans. (2004) 3927, and references therein.

[3] T.R. Spalding, B. O'Leary, L. Neville, G. Ferguson, in: M. Davidson, A.K. Hughes, T.B. Marder, K. Wade (Eds.), Contemporary Boron Chemistry, Special Publication No. 253, Royal Society of Chemistry, 2000, p. 92.

[4] B.J. O'Leary, D.M. Murphy, T.R. Spalding, G.F. Ferguson, J. Organomet. Chem. 526 (1996) 195.

[5] A.T. O'Dowd, T.R. Spalding, G.F. Ferguson, J.F. Gallagher, D. Reed, J. Chem. Soc., Chem. Commun. (1993) 1816.

[6] L.A. Neville, T.R. Spalding, G. Ferguson, Angew. Chem., Int. Ed. 39 (2000) 3598.

[7] A.G. Avent, S.E. Lawrence, M.M. Meehan, T.G. Russell, T.R. Spalding, Collect. Czech. Chem. Commun. 67 (2002) 1051.

[8] F.J. Feher, T.A. Budzichowski, J.W. Ziller, Inorg. Chem. 31 (1992) 5100.

[9] O. Graalmann, U. Klingebiel, W. Clegg, M. Haase, G.M. Sheldrick, Z. Anorg. Allg. Chem. 519 (1984) 87.

[10] F.H. Allen, O. Kennard, D.G. Watson, L. Brammer, A.G. Orpen, R. Taylor, J. Chem. Soc., Perkin Trans. II (1987) S1.

[11] B.J. O'Leary, Ph.D. Thesis, University College Cork, National University of Ireland, Cork, Ireland, 1998.

[12] D. Murphy, J.P. Sheehan, T.R. Spalding, G. Ferguson, A.J. Lough, J.F. Gallagher, J. Mater. Chem. 3 (1993) 1275.

[13] B.J. Brisdon, M.F. Mahon, K.C. Molloy, P.J. Scholfield, J. Organomet. Chem. 435 (1992) 11.

[14] D.A. Foucher, A.J. Lough, I. Manners, Inorg. Chem. 31 (1992) 3034.

[15] G. Ferguson, A.J. Lough, J.P. Sheehan, T.R. Spalding, Acta Crystallogr., Sect. C 47 (1991) 379.

[16] G. Ferguson, J.F. Gallagher, D. Murphy, J.P. Sheehan, T.R. Spalding, Polyhedron 12 (1993) 859.

[17] N. Winkhofer, H.W. Roesky, M. Noltemeyer, W.T. Robinson, Angew. Chem., Int. Ed. 31 (1992) 599.

[18] E.J. Gabe, Y. Le Page, J.-P. Charland, F.L. Lee, P.S. White, J. Appl. Crystallogr. 22 (1989) 384.

[19] S. Mackay, W. Dong, C. Edwards, A. Henderson, C.J. Gilmore, N. Stewart, K. Shankland, A. Donald, maXus, University of Glasgow, Glasgow, Scotland, 1998.

[20] G.M. Sheldrick, Acta Crystallogr., Sect. A 46 (1990) 467.

[21] A.L. Spek, PLATON, University of Utrecht, Utrecht, Holland, 2002.

[22] G.M. Sheldrick, SHELXL-97, University of Göttingen, Göttingen, Germany, 1997.